The application of multi-layer phosphor-in-glass sheets in boosting white light emitting diodes chromaticity

Ha Thanh Tung[1], Huu Phuc Dang[2], Nguyen Le Thai[3]
[1]Faculty of Basic Sciences, Vinh Long University of Technology Education, Vinh Long Province, Vietnam
[2]Faculty of Fundamental Science, Industrial University of Ho Chi Minh City, Ho Chi Minh City, Vietnam
[3]Faculty of Engineering and Technology, Nguyen Tat Thanh University, Ho Chi Minh City, Vietnam

Article Info	ABSTRACT
	With the use of phosphor-in-glass (abbreviated as PiG), it is possible to make alterations for the remote adjustment incorporated with a diode that generates blue light emitting diode (LED) and acquire remarkably superior light output at considerable temperatures of color compared to standard structures of LED devices. It should be noted that the imbrication of emission spectra in phosphor substances, as well as the forfeited, amount of light caused by re-absorption appear to be the primary problems stemming from the model of multi-color phosphor. The earlier study came up with the method of creating various phosphor-in-glass (PiGs) by slicing and reconstruction, which remedied certain aspects of the flaws mentioned. Practically speaking, the light amount forfeited occurs in the linking zones in the middle of the color phosphor and will be a subject of the research. We can see for certain that it is necessary to come up with a means of preparation to deal with the issues of the interfacial layer. Therefore, the low sintering of PiGs at 600 °C was considered an appropriate procedure, as it could create a double-layer PiG in a lying direction as well as a triple-layer PiG yielding superior optical efficiency when compared to equivalent versions.

Corresponding Author:

Huu Phuc Dang
Faculty of Fundamental Science, Industrial University of Ho Chi Minh City
No. 12 Nguyen Van Bao Street, Ho Chi Minh City, Vietnam
Email: danghuuphuc@iuh.edu.vn

1. INTRODUCTION

The phosphor-converted diode that generates white light (abbreviated as WLED) has recently been shown to have many benefits including great efficacy, longevity, productive power usage, as well as improved measurements. Therefore, it could be deemed the most promising optical enhancement for the field of luminescence. The researches carried out not long ago to innovate the white light emitting diodes (WLEDs) apparatuses drastically influenced the application of phosphor substances, models, packaging methods, as well as encapsulants [1]–[4]. In a standard way, we generate the white light by mixing various light sources (for example, $Y_3Al_5O_{12}:Ce^{3+}$ incorporated with resin substance and a blue-chip of LED). It is most commonly used thanks to its effectiveness, but this outdated technique, on the other hand, yields inferior thermal efficacy and hence could impede optical propagation and degrade the lumen efficiency. This is especially true for high-power apparatuses. The mentioned technique can yield significant heat and deteriorate the quality of color and harm the inner parts of apparatuses [5]–[7]. Researches on remote phosphor structures with phosphor ceramics, luminescent glasses, and PiG. as its basis, were carried out to find a way to solve the flaws [6]–[10]. In the end, there were researches that looked into the LED structures with a gap separating material sheets and achieved outstanding enhancement (from 20% to 30%) when compared to the conformal structure that has identical parts

[11]–[13]. While the difficult preparation procedure usually discourages the use of phosphor ceramics with plate-shaped phosphor particles, the ceramics is still very valuable for their capability of augmenting the color-converting process in luminescent glass. It is worth noting that phosphor ceramics and luminescent glasses could be replaced by PiGs that are receiving more attention from researchers for their equivalent performance. After sintering the phosphors combined with glass, the PiGs resulting from the process can yield a stable performance, regardless of the LED's state. Because of this, to achieve further improvement, researchers focused on the parameters that were formerly ignored and could influence the optical efficacy, which includes the thickness and position of layers intended for converting color [6], [14]. After selection, the combination of phosphor articles of many green, yellow and red phosphors is made to boost the WLEDs' chromaticity. But the spectral imbrication resulting from an arbitrary combination of the phosphors impairs the apparatus' light output and leads to inferior chromaticity as well as emission efficacy [15], [16]. To remedy this flaw, the PiG model created by piling up sheets of green/yellow and red is set aside in favor of the multi-color 4-quadrant-type PiG that can alternate colors [17], [18]. With the technique mentioned, it is possible to alter the chromaticity by aligning the color substances. The complete lack of reabsorption can certainly result in greater optical efficacy for the WLEDs than phosphor-in-glass (PiGs) created by arbitrary mixtures. We should be noted that for such models, the empty space at the interface of the overlapped plate as well as the alternate quadrants, understood as the scattering layer, can lead to a considerably inferior enhancement if compared to desired results [19], [20]. In the case of the overlapped PiG, the chip of LED generates the blue light that bypasses the empty space of the central layer, reducing the final light amount generated. For the 4-quadrant PiG, the empty space separating the alternate quadrants can reduce the optical efficacy as well through blue light scattering. In addition, it is exceptionally complex to apply this method for widespread practical use, thus making it unsuitable for mass production [21], [22]. As these results are known, the PiG model, as well as its preparation procedure, was modified for this research so that we could entirely avoid the flaws in optical efficacy. PiGs implemented with the commercial $Lu_3Al_5O_{12}:Ce^{3+}$ (LuAG:Ce^{3+}) and $CaAlSiN_3:Eu^{2+}$ (CASN:Eu^{2+}) phosphors are created through a procedure that involves only a single step without piling up or further modifying the sheets that are created before. By conducting experiments, we can assess how we can utilize the multi-layer or multi-segment PiGs with WLEDs' remote structure. In addition, the research will examine the correlation between the PiGs spectral emission and the angle of light. The technique mentioned in this research could help with alternation of optical characteristics, such as the temperature of color and color rendering index (CRI).

2. RESEARCH PROCEDURE

2.1. The creation process of phosphor substances

This section describes the task of creating the phosphors for the experiments. The first phosphor to be prepared is the green phosphor $Gd_2O_2S:Pr^{3+}$. Mix the ingredients Gd_2O_3 and Pr_6O_{11} with nitric acid until a precipitant is seen. The concoction is then heated at the temperature of 1,000 °C. Mix the oxide with sulfur and $NaCO_3$ and heat the concoction at 1,100 °C. Once the heating is done, the resulting substance is to be rinsed in water and combined with Ce for fewer afterglows. The resulting phosphor will have the emission color of green with an emission peak of 510 nm. The chemical composition of the phosphor is shown in Table 1.

The creation of the red phosphor $Na_{1.23}K_{0.42}Eu_{0.12}TiSi_5O_{13}$'$xH_2O:Eu^{3+}$ will be described in detail in this part. The process begins with creating ETS-10. Combine sodium silicate solution with NaCl and KLC in 20 g of water. The concoction is to be stirred, then combined with anatase. Disinfect the concoction under autogenous pressure at the temperature of 230 °C for 24 hours. The substance acquired is to be filtered rinsed in pure water at room temperature and let dry at 110 °C. The process continues with creating the Eu^{3+} doped ETS-10. Combine 3,94 g of ETS-10 made previously with the concoction of 0.07 g $Eu(NO_3)_3 \cdot 5H_2O$ and 250 ml of water. The concoction is to be stirred for 24 hours and kept at the temperature of 60 °C. Filter the result and let it dry at the temperature of 110 °C. The same process can be applied to the last two materials. The acquired red phosphor $Na_{1.23}K_{0.42}Eu_{0.12}TiSi_5O_{13}$'$xH_2O:Eu^{3+}$ generates red light and has an emission peak of 2.00 eV. The chemical composition of $Na_{1.23}K_{0.42}Eu_{0.12}TiSi_5O_{13}$'$xH_2O:Eu^{3+}$ can be seen in Table 2.

Table 2. Chemical composition of red phosphor $Na_{1.23}K_{0.42}Eu_{0.12}TiSi_5O_{13}$'$xH_2O:Eu^{3+}$

Ingredient	Mole %	By weight (g)
Sodium silicate solution (8% Na_2O; 27% SiO_2; 65% H_2O)	30.7 (of Si)	20.0
TiO_2 (Anatase)	5.6 (of Ti)	1.30
NaCl	58.1 (of Na)	6.90
KCl	5.6 (of K)	1.30
$Eu(NO_3)_3 \cdot 5H_2O$	0.12 (of Eu)	0.15

2.2. Model recreation

For the experiments, the PiGs utilized are made by sintering the glass under low-melting-point ($\leq$ 600°C). The SiO_2, B_2O_3, ZnO, Al_2O_3, and K_2O created the (SiO_2, B_2O_3, ZnO)-Al_2O_3, K_2O system; SiO_2, B_2O_3, and ZnO accounted for 25, 25, and 30 wt.%, respectively, and hence a total portion of 80 wt.%. K_2O and Al_2O_3 accounted for the remaining portions of 15 and 5 wt.% respectively. These are the chemical composition of glass frit [8]. The PiGs is made by combining an appropriate amount of glass frits with commercial powders of $LuAG:Ce^{3+}$ and $CASN:Eu^{2+}$ [19]. After combining, the acquired substance is heated at the temperature of 600ºC to yield the result. In all of the PiGs shown in the next parts, the presence of green phosphor $LuAG:Ce^{3+}$ is doubled compared to that of red phosphor $CASN:Eu^{2+}$ while the proportions of each phosphor to glass were respectively 2:10 and 1:10. Once the green and red PiG mentioned are made, we positioned them as a pair of horizontal layers or four quadrants on a PiG. As a result, every PiG's color is decided by the phosphor type placed in the PiG. These procedures, which involve only a single step, are intended to create the PiGs shown below. Based on the model of stacked phosphor adjustment, we crafted the double-layer reference PiGs [23]. We crafted the 4-quadrant PiG by repositioning the colored section of the PiGs, shown in our earlier researches [24]. To carry out such a task, we cut the slice the PiGs into four identical pieces and reposition them. To create the red and green PiGs, we combined phosphor $CASN:Eu^{2+}$ or phosphor $LuAG:Ce^{3+}$, which generated red and green light respectively, with an amount of glass frit prepared beforehand, then heated the substance at the temperature of 600 ºC to harden it. We left two-quadrant parts (each was 250 mm in diameter and 1-mm thick) in a round sheet and supported them using a glass substrate that was optically inert.

Figure 1 shows the dual-layer phosphor (DL) and triple-layer phosphor (TL) structures. The DL structure consists of a red phosphor layer on top of a yellow phosphor layer, see Figure 1(a). The TL structure is similar to DL but has the green phosphor layer in the middle, as shown in Figure 1(b). The layers of phosphor are always 0.08-meter thick. Furthermore, the phosphor $YAG:Ce^{3+}$ concentration is modified in response to the changes in the concentration of the red or green phosphor so that the average correlated color temperature (ACCTs) is kept at a moderate level. Also, for each ACCT, every phosphor package has various concentrations of phosphor $YAG:Ce^{3+}$, resulting in many different dispersion attributes of the WLEDs. Such disparity can also create variations in optical features.
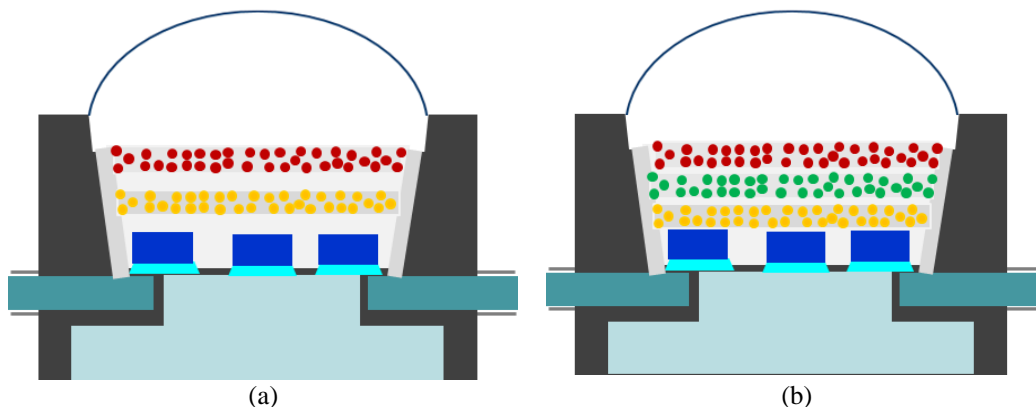

Figure 1. Illustration of multi-layer phosphor structures of white LEDs: (a) dual-layer phosphor (DL) and (b) triple-layer phosphor (TL)

As we can see in Figure 2, the concentration of yellow phosphor in the DL package is greater compared to the TL package, regardless of ACCTs. In case every package has identical ACCT, when the concentration of phosphor $YAG:Ce^{3+}$ increases, back-scattering will occur more frequently, resulting in a lower lumen generated, see Figure 2(a). This will also cause a lack of color homogeneity between the three colors (yellow, red, and green) that are used to generate white light, resulting in inferior chromaticity. From here, we can see that the increased back-scattering can negatively affect the lumen as well as the color performance in WLEDs, and to solve the problem, we need to boost the red-light element in order to lower the back-scattering, as shown in Figure 2(b). The aforementioned data indicated that the three-layer phosphor package appears to be the best choice when it comes to controlling the light characteristics. To verify such a claim, it is necessary to present more important information on the phosphor packages and emission spectrum, as displayed in Figure 3.
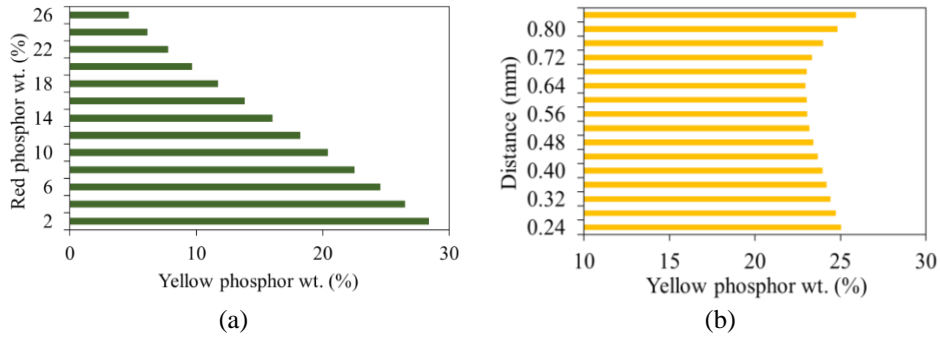
(a)   (b)

Figure 2. The concentration of yellow YAG:Ce^{3+} phosphor in each remote phosphor structure at each different ACCT: (a) DL and (b) TL
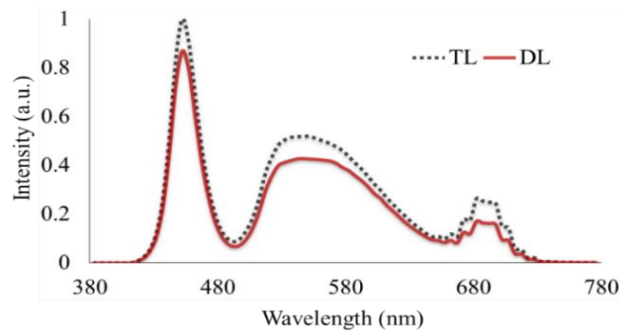

Figure 3. Emission spectra of phosphor configurations

3. RESULTS AND ANALYSIS

Figure 4 compares the CRI values of dual-layer (DL) and triple-layer (TL) remote phosphor packages. From there, it is obvious that the DL package has better CRI values compared to the TL package, regardless of ACCT, see Figure 4(a). Furthermore, the DL's CRI value is at its highest when the ACCT is 8,500 K, as shown in Figure 4(b). This outcome can be very significant for the goal of achieving higher CRI in remote phosphor structure as it is not an easy task to manipulate CRI at high ACCT (more than 7,000 K). With the implementation of the layer of red phosphor $Mg_8Ge_2O_{11}F_2$:Mn^{4+} to generate additional red-light presence, the DL package could reach the greatest CRI value. Thanks to this, the DL package is most beneficial to the mass production of high-CRI WLEDs. It should be noted that CRI cannot assess chromaticity in the best way. For this reason, CQS, a parameter developed to take three aspects into account, including CRI, beholder's taste, and color coordinate, has seen considerable recognition and application in studies. Thanks to the multiple aspects concerned, CQS can assess the color quality in WLEDs to a greater extent. Figure 5 demonstrates the CQS comparison between the remote phosphor packages. The TL package appears to yield the best CQS value, thanks to color uniformity between the yellow, green and red colors. The CQS value is dependent on the chromaticity, indicating that the TL can benefit the lumen as well as the chromaticity performance thanks to the increased presence of red and green light.

In Figure 5, the TL package appears to have the best performance in the quality of color. But the problem is we do not know if such quality of color could result in a loss of light generated. In order to verify such concern, we made a comparison between the lumen values of both structures and utilized formulas to demonstrate the propagated blue light and transmuted yellow light [25]:

$$PB_2 = PB_0 e^{-\alpha_{B_2}h} e^{-\alpha_{B_2}h} = PB_0 e^{-2\alpha_{B_2}h} \tag{1}$$

$$PY_2 = \frac{1}{2}\frac{\beta_2 PB_0}{\alpha_{B_2}-\alpha_{Y_2}}[e^{-\alpha_{Y_2}h} - e^{-\alpha_{B_2}h}]e^{-\alpha_{Y_2}h} + \frac{1}{2}\frac{\beta_2 PB_0}{\alpha_{B_2}-\alpha_{Y_2}}[e^{-\alpha_{Y_2}h} - e^{-\alpha_{B_2}h}]$$
$$= \frac{1}{2}\frac{\beta_2 PB_0}{\alpha_{B_2}-\alpha_{Y_2}}[e^{-2\alpha_{Y_1}h} - e^{-2\alpha_{B_1}h}] \tag{2}$$

The formulas below demonstrate the propagated blue light and transmuted yellow light in the remote phosphor structure with the layer of phosphor that is $\frac{2}{3}$ h thick:

$$PB_3 = PB_0 . e^{-\alpha_{B_2}\frac{2h}{3}} . e^{-\alpha_{B_2}\frac{2h}{3}} . e^{-\alpha_{B_2}\frac{2h}{3}} = PB_0 . e^{-2\alpha_{B_3}h} \tag{3}$$

$$\begin{aligned} PY'_3 &= \frac{1}{2}\frac{\beta_3 PB_0}{\alpha_{B_3}-\alpha_{Y_3}}\left[e^{-\alpha_{Y_3}\frac{2h}{3}} - e^{-\alpha_{B_3}\frac{2h}{3}}\right] e^{-\alpha_{Y_3}\frac{2h}{3}} + \frac{1}{2}\frac{\beta_3 PB_0 e^{-\alpha_{B_3}\frac{2h}{3}}}{\alpha_{B_3}-\alpha_{Y_3}}\left[e^{-\alpha_{Y_3}\frac{2h}{3}} - e^{-\alpha_{B_3}\frac{2h}{3}}\right] \\ &= \frac{1}{2}\frac{\beta_3 PB_0}{\alpha_{B_3}-\alpha_{Y_3}}\left[e^{-\alpha_{Y_3}\frac{4h}{3}} - e^{-2\alpha_{B_3}\frac{4h}{3}}\right] \end{aligned} \tag{4}$$

$$\begin{aligned} PY_3 &= PY'_3 . e^{-\alpha_{Y_3}\frac{2h}{3}} + PB_0 . e^{-2\alpha_{B_3}\frac{4h}{3}}\frac{1}{2}\frac{\beta_3}{\alpha_{B_3}-\alpha_{Y_3}}\left[e^{-\alpha_{Y_3}\frac{2h}{3}} - e^{-\alpha_{B_3}\frac{2h}{3}}\right] \\ &= \frac{1}{2}\frac{\beta_3 PB_0}{\alpha_{B_3}-\alpha_{Y_3}}\left[e^{-\alpha_{Y_3}\frac{4h}{3}} - e^{-\alpha_{B_3}\frac{4h}{3}}\right] e^{-\alpha_{Y_3}\frac{2h}{3}} + \frac{1}{2}\frac{\beta_3 PB_0 e^{-\alpha_{B_3}\frac{4h}{3}}}{\alpha_{B_3}-\alpha_{Y_3}}\left[e^{-\alpha_{Y_3}\frac{2h}{3}} - e^{-\alpha_{B_3}\frac{2h}{3}}\right] \\ &= \frac{1}{2}\frac{\beta_3 PB_0}{\alpha_{B_3}-\alpha_{Y_3}}\left[e^{-\alpha_{Y_3}h} - e^{-2\alpha_{B_3}h}\right] \end{aligned} \tag{5}$$

For the formulas presented, h indicates the thickness of a phosphor layer. The two-layer and three-layer structures are indicated by the small numbers "1" and "2" located below the letters respectively. The conversion coefficient of the conversion of blue light to yellow light is represented by the symbol β. The reflection coefficient of the yellow light is represented by the symbol γ. The blue light and yellow light intensities are represented by the symbols PB and PY respectively or represented by the symbol PB_0 as a whole. The symbols αB and αY indicate small portions of the energy amount wasted of blue and yellow light in the transmission process of the layer of phosphor. The PY'_3 symbol represents the propagated yellow light bypassing the pair of phosphor layers.

The formula below displays the superiority of the three-layer phosphor package in improving the pc-LEDs' optical efficacy in comparison to the two-layer package:

$$\frac{(PB_3 - PY_3) - (PB_2 + PY_2)}{(PB_2 + PY_2)} > \frac{e^{-2\alpha_{B_3}h} - e^{-2\alpha_{B_2}h}}{e^{-2\alpha_{Y_3}h} - e^{-2\alpha_{B_2}h}} \tag{6}$$

From the presented relationship of the components with the angle, we can see the association of the location of components with the optical emission wavelength range. Although the dispersion of huge wavelengths in the spectrum is consistent, the efficiency of lesser wavelengths depends on the angle. In addition, the green component's alternating dispersion pattern along with the sudden shift of blue component dispersion is caused by many aspects. Such aspects may include particle dispersion of the component wavelengths, the segmented sheets' relative transparency, and the material sheets' position. The identical amount and location of the green and red phosphors of LuAG:Ce^{3+} and CASN:Eu^{2+} can help prove the aforementioned speculation. Furthermore, from the attributes of the light rays dispersing at huge angles but not the small ones, it is obvious that the proportion of phosphor to glass for every material sheet has an impact on the chromatic intensity dispersion of the adjustment.

Figure 6 shows the change of luminous flux when changing phosphor concentration for both DL and TL structures. From the outcomes acquired, it seems possible to eliminate the close relationship with the angle shown before through the task of improving the PiG's creation procedure. Specifically, we should evaluate the corresponding intensity of the blue light, rather than attempt to modify the proportion of green phosphor to red phosphor in the corresponding sections to manipulate the color release, see Figure 6(a). In order to acquire a bright green light as well as to lower the blue light's translucency in the spectra, we can use the green phosphor LuAG:Ce^{3+} mixed with glass due to its greater amount of phosphor particles. The chromatic elements' relative intensity dispersion at different opposite angles can help verify this. In the PiG's green zone, the insignificant concentration of phosphor can diminish the blue light's relationship with the angle, as the escaped blue light dominates the concentrations of phosphor, as displayed in Figure 6(b). The increase in escaped light can be advantageous to the relationship of both green and blue elements with the angle. On the other hand, the blue light is usually ignored due to the fact that it is converted by the layer of green phosphor for the most part. It is worth noting that the blue element achieves the greatest intensity in the presence of red elements generated by the color sheet. In such a case, the proportion of red phosphor to green phosphor is 1:2, and hence the propagation of the blue light generated through the red zone. As a result, the green and blue zones with great intensity occur in the polar chart's alternating quadrants. From such outcomes, it is clear that the remote structure can productively regulate the attributes of the spectrum. Therefore, it becomes the better choice for

contemporary WLEDs models compared to the standard packaging of LED. From here, we can boost the CIE by using the appropriate structure as well as the creation process, rather than just optimizing parameters (thickness, for example). The close relationship between the light output and angle is related to the substance of PiG and PiG's attributes of light. On the other hand, with the model and creation process that form the PiG's layers and divide the spaces between them, it is possible to develop better-LED versions as well as adjustable attributes of light, see Figure 7. We can split the quadruple-section PiG into eight identical parts, in which we can leave a segment angle with a particular color at the angle of 45º in the center. With the relationship between the color elements and the angle diminished, we can enhance the cold light to a greater extent. In case the emission from the blue chips of LED alternatively generates a light that is dependent on the angle but not light with uniform dispersion, it will result in different values of the relative angular width of the alternate-color sections.
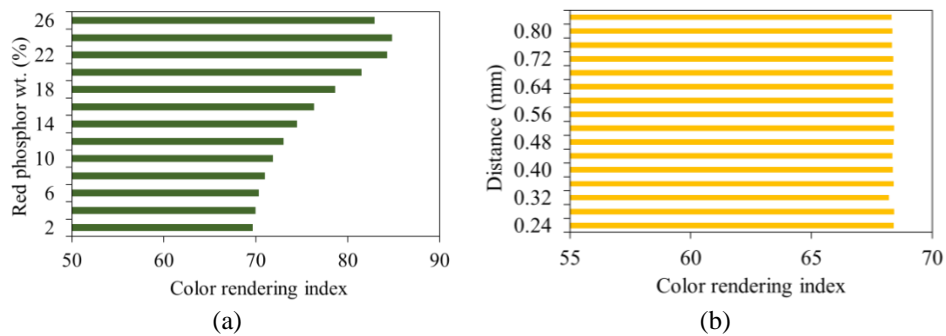
Figure 4. Color rendering indexes of phosphor configurations corresponding to ACCTs: (a) DL and (b) TL
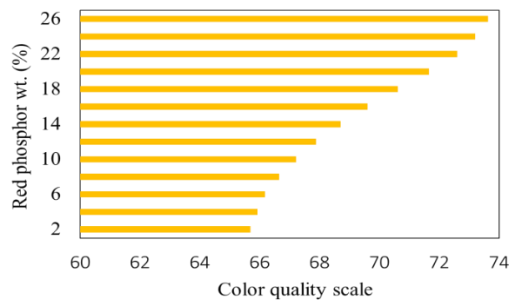
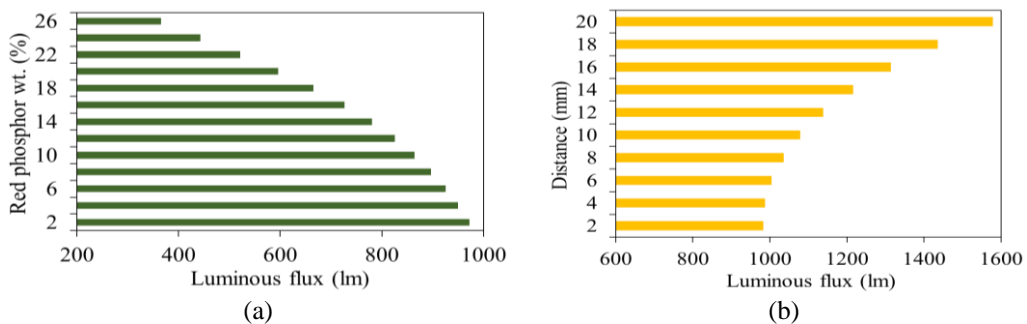Figure 5. Color quality scale of phosphor configurations corresponding to ACCTs

Figure 6. Luminous output (LO) of phosphor configurations corresponding to ACCTss: (a) DL and (b) TL
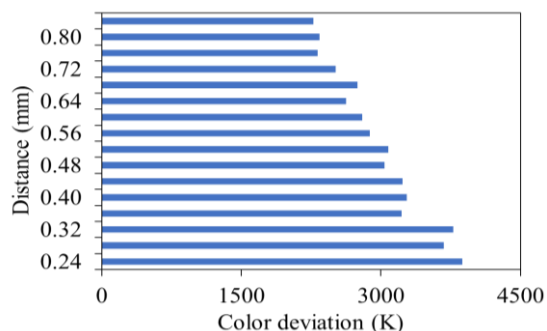
Figure 7. Correlated color temperature deviation (D-CCT) of remote phosphor configurations corresponding to ACCTs

4.   CONCLUSION

The model and the creation process of the PiG, which is recommended in this study, involve a single-step creation procedure that can help eliminate entirely the reabsorption of the green light generated, which is the result of the red element of high-power WLEDs. With such a technique, it is also possible to minimize the light that escapes from the InGaN chip located at the linking surface of the material sheets. The technique above yielded beneficial outcomes when we compared the double-layer with triple-layer structures, each implemented with red $CASN:Eu^{2+}$ and $LuAG:Ce^{3+}$ green PiG which was prepared using different ingredients. Furthermore, our examination authenticated the ability of the adjustment mentioned to lessen the relationship between WLEDs' luminescence and the angle and to boost the chromatic homogeneity at the 90° angle maximumly. We could raise the number of sections to diminish the chromatic deviation further. Thanks to our in-depth study, we have managed to yield such desirable results and came up with the technology that can augment high-power WLEDs devices.

REFERENCES

[1]   J. Chen *et al*., "Fabrication of (Tb,Gd) 3 Al 5 O 12 :Ce 3+ phosphor ceramics for warm white light-emitting diodes application ," *Optical Materials Express*, vol. 9, no. 8, p. 3333, Aug. 2019, doi: 10.1364/ome.9.003333.
[2]   B. Fond, C. Abram, M. Pougin, and F. Beyrau, "Investigation of the tin-doped phosphor (Sr,Mg) 3 (PO 4) 2 :Sn 2+ for fluid temperature measurements ," *Optical Materials Express*, vol. 9, no. 2, p. 802, Feb. 2019, doi: 10.1364/ome.9.000802.
[3]   Z. Li, J. Zheng, J. Li, W. Zhan, and Y. Tang, "Efficiency enhancement of quantum dot–phosphor hybrid white-light-emitting diodes using a centrifugation-based quasi-horizontal separation structure," *Optics Express*, vol. 28, no. 9, p. 13279, Apr. 2020, doi: 10.1364/oe.392900.
[4]   H. S. El-Ghoroury, Y. Nakajima, M. Yeh, E. Liang, C. L. Chuang, and J. C. Chen, "Color temperature tunable white light based on monolithic color-tunable light emitting diodes," Optics Express, vol. 28, pp. 1206–1215, 2020, doi: 10.1364/OE.375320.
[5]   X. Xi *et al.,* "Chip-level Ce:GdYAG ceramic phosphors with excellent chromaticity parameters for high-brightness white LED device," *Optics Express*, vol. 29, no. 8, p. 11938, Apr. 2021, doi: 10.1364/oe.416486.
[6]   S. Xu *et al*., "Exploration of yellow-emitting phosphors for white LEDs from natural resources," *Applied Optics*, vol. 60, no. 16, p. 4716, Jun. 2021, doi: 10.1364/ao.424108.
[7]   G. Zhang, K. Ding, G. He, and P. Zhong, "Spectral optimization of color temperature tunable white LEDs with red LEDs instead of phosphor for an excellent IES color fidelity index," *OSA Continuum*, vol. 2, no. 4, p. 1056, Apr. 2019, doi: 10.1364/osac.2.001056.
[8]   P. D. Huu and M. H. N. Thi, "Enhancing optical properties of WLEDs with LaOF:Eu3+&SiO2 application," *Bulletin of Electrical Engineering and Informatics*, vol. 11, no. 1, pp. 143–149, Feb. 2022, doi: 10.11591/eei.v11i1.2910.
[9]   W. Zhong, J. Liu, D. Hua, S. Guo, K. Yan, and C. Zhang, "White LED light source radar system for multi-wavelength remote sensing measurement of atmospheric aerosols," *Applied Optics*, vol. 58, no. 31, p. 8542, Nov. 2019, doi: 10.1364/ao.58.008542.
[10]   T. Y. Orudzhev, S. G. Abdullaeva, and R. B. Dzhabbarov, "Increasing the extraction efficiency of a light-emitting diode using a pyramid-like phosphor layer," *Journal of Optical Technology*, vol. 86, no. 10, p. 671, Oct. 2019, doi: 10.1364/jot.86.000671.
[11]   N. C. Abd Rashid *et al.,* "Spectrophotometer with enhanced sensitivity for uric acid detection," *Chinese Optics Letters,* vol. 17, no. 8, p. 081701, 2019, doi: 10.3788/col201917.081701.
[12]   C. Huang, Y. Chang, L. Han, F. Chen, S. Li, and J. Hong, "Bandwidth correction of spectral measurement based on Levenberg–Marquardt algorithm with improved Tikhonov regularization," *Applied Optics*, vol. 58, no. 9, p. 2166, Mar. 2019, doi: 10.1364/ao.58.002166.
[13]   Y. Zhou *et al.,* "Comparison of nonlinear equalizers for high-speed visible light communication utilizing silicon substrate phosphorescent white LED," *Optics Express*, vol. 28, no. 2, p. 2302, Jan. 2020, doi: 10.1364/oe.383775.
[14]   H. Li *et al.,* "Electrically driven, polarized, phosphor-free white semipolar (20-21) InGaN light-emitting diodes grown on semipolar bulk GaN substrate," Optics Express, vol. 28, no. 9, p. 13569, Apr. 2020, doi: 10.1364/oe.384139.
[15]   A. Ali *et al.,* "Blue-laser-diode–based high CRI lighting and high-speed visible light communication using narrowband green-/red-emitting composite phosphor film," *Applied Optics*, vol. 59, no. 17, p. 5197, Jun. 2020, doi: 10.1364/ao.392340.
[16]   J. O. Kim, H. S. Jo, and U. C. Ryu, "Improving CRI and scotopic-to-photopic ratio simultaneously by spectral combinations of CCT-tunable LED lighting composed of multi-chip LEDs," *Optica*, pp. 247–252, 4AD, doi: 10.1364/COPP.4.000247.

[17] W.-C. Wang, C.-H. Cheng, H.-Y. Wang, and G.-R. Lin, "White-light color conversion with red/green/violet laser diodes and yellow light-emitting diode mixing for 34.8 Gbit/s visible lighting communication," *Photonics Research*, vol. 8, no. 8, p. 1398, Aug. 2020, doi: 10.1364/prj.391431.

[18] D. T. Tuyet *et al.,* "Deep red fluoride dots-in-nanoparticles for high color quality micro white light-emitting diodes," *Optics Express*, vol. 28, no. 18, p. 26189, Aug. 2020, doi: 10.1364/OE.400848.

[19] M. Talone and G. Zibordi, "Spatial uniformity of the spectral radiance by white LED-based flat-fields," *OSA Continuum*, vol. 3, no. 9, p. 2501, Sep. 2020, doi: 10.1364/OSAC.394805.

[20] H.-K. Shih, C.-N. Liu, W.-C. Cheng, and W.-H. Cheng, " High color rendering index of 94 in white LEDs employing novel CaAlSiN 3 : Eu 2+ and Lu 3 Al 5 O 12 : Ce 3+ co-doped phosphor-in-glass ," *Optics Express,* vol. 28, no. 19, p. 28218, Sep. 2020, doi: 10.1364/oe.403410.

[21] Y. Ma *et al*., "Broadband emission Gd 3 Sc 2 Al 3 O 12 :Ce 3+ transparent ceramics with a high color rendering index for high-power white LEDs/LDs ," *Optics Express*, vol. 29, no. 6, p. 9474, Mar. 2021, doi: 10.1364/oe.417464.

[22] S. Feng and J. Wu, "Color lensless in-line holographic microscope with sunlight illumination for weakly-scattered amplitude objects," *OSA Continuum*, vol. 2, no. 1, p. 9, Jan. 2019, doi: 10.1364/osac.2.000009.

[23] A. J. Henning, J. Williamson, H. Martin, and X. Jiang, "Improvements to dispersed reference interferometry: beyond the linear approximation," *Applied Optics*, vol. 58, no. 1, p. 131, Jan. 2019, doi: 10.1364/ao.58.000131.

[24] R. Deeb, J. V. D. Weijer, D. Muselet, M. Hebert, and A. Tremeau, "Deep spectral reflectance and illuminant estimation from self-interreflections," *Journal of the Optical Society of America A*, vol. 36, no. 1, p. 105, Jan. 2019, doi: 10.1364/josaa.36.000105.

[25] S. Kumar, M. Mahadevappa, and P. K. Dutta, "Extended light-source-based lensless microscopy using constrained and regularized reconstruction," *Applied Optics*, vol. 58, no. 3, p. 509, Jan. 2019, doi: 10.1364/ao.58.000509.

BIOGRAPHIES OF AUTHORS

Ha Thanh Tung received the PhD degree in physics from University of Science, Vietnam National University Ho Chi Minh City, Vietnam, he is working as a lecturer at the Faculty of Basic Sciences, Vinh Long University of Technology Education, Vietnam. His research interests focus on developing the patterned substrate with micro- and nano-scale to apply for physical and chemical devices such as solar cells, OLEDs, and photoanode. He can be contacted at email: tunght@vlute.edu.vn

Huu Phuc Dang is Associate Professor at college of Electrical & Mechanical Engineering, National University of Sciences and Technology, Pakistan. He Holds a PhD degree in Computer Engineering with specialization in medical image analysis. His research areas are image/signal processing, biometrics, medical image analysis and pattern recognition. He is director of Biomedical Image and Signal Analysis Research Lab. He is a recipient of different national and international awards such as NUST overall best researcher award, HEC Best University Teacher Award, C EME NUST best researcher award, HEC best research scholar award, Pakistan software house association awards (P@SHA), Asia Pacific ICT alliance awards (APICTA) etc. He is cofounder of RISETech which is a technology-based company and their innovative products received appreciation at national and international level. Dr Usman has filed a number of patents and industrial designs on his innovative ideas and has been awarded with two international patents. His research interests include image/signal processing, biometrics, medical image and analysis, and pattern recognition. He can be contacted at email: Usman.akram@ceme.nust.edu.pk.

Nguyen Le Thai received his BS in Electronic engineering from Danang University of Science and Technology, Vietnam, in 2003, MS in Electronic Engineering from Posts and Telecommunications Institute of Technology, Ho Chi Minh, Vietnam, in 2011 and PhD degree of Mechatronics Engineering from Kunming University of Science and Technology, China, in 2016. He is a currently with the Nguyen Tat Thanh University, Ho Chi Minh City, Vietnam. His research interests include the renewable energy, optimisation techniques, robust adaptive control and signal processing. He can be contacted at email: nlthai@nttu.edu.vn.